

Germafluorenes: New Heterocycles for Plastic Electronics

Nicolas Allard,[†] Réda Badrou Aïch,^{†,‡} David Gendron,[†] Pierre-Luc T. Boudreault,[†]
Christian Tessier,[§] Salima Alem,[‡] Shing-Chi Tse,[‡] Ye Tao,[‡] and Mario Leclerc^{*,†}

[†]Contribution from Canada Research Chair on Electroactive and Photoactive Polymers. Département de Chimie, Université Laval, Quebec City, Quebec, Canada, G1V 0A6, [‡]Institute of Microstructural Sciences, National Research Council of Canada, Ottawa, Ontario, Canada, K1A 0R6, and [§]Département de Chimie, Université Laval, Quebec City, Quebec, Canada, G1V 0A6

Received November 23, 2009; Revised Manuscript Received January 11, 2010

ABSTRACT: The synthesis and characterization of new heterofluorene derivatives based on germanium are described. These germafluorene monomers have been polymerized with different aromatic comonomers. The resulting homopolymers and alternating copolymers have been characterized by size exclusion chromatography, thermal analyses (TGA and DSC), UV–vis–NIR absorption spectroscopy, X-ray diffraction, and cyclic voltammetry. These homopolymers and copolymers are air-stable and present bandgaps ranging from 3.0 to 1.6 eV. Some copolymers were tested in field-effect transistors (FETs) and bulk heterojunction photovoltaic cells (PCs). Best results in FETs were obtained with poly[2,7-(9,9-di-*n*-butylgermafluorene)-*alt*-3,6-bis(thiophen-5-yl)-2,5-dioctylpyrrolo[3,4-*b*]pyrrole-1,4-dione], which shows a hole mobility up to 0.04 cm² (V·s)^{−1} with an $I_{\text{on}}/I_{\text{off}}$ ratio of 1.0×10^6 . For photovoltaic applications, the best results were obtained with poly[2,7-(9,9-di-*n*-octylgermafluorene)-*alt*-5,5-(4',7'-di-2-thienyl-2',1',3'-benzothiadiazole)] with a power conversion efficiency (PCE) of 2.8%.

1. Introduction

Great advances have been achieved over the past decade regarding the synthesis of new conjugated polymers for field-effect transistors (FETs)¹ and photovoltaic cells (PCs).² For instance, recent developments on FETs by Müllen et al. have shown that it is possible to reach a hole mobility above 1.0 cm² (V·s)^{−1} by using a cyclopentadithiophene–benzothiadiazole copolymer.³ The donor–acceptor architecture of this copolymer gives a relatively low bandgap, which is another important parameter for photovoltaic applications. When used as the active layer in a bulk heterojunction (BHJ) solar cell, this particular polymer reached a power conversion efficiency (PCE) as high as 5.5%.⁴ Along these lines, several other donor–acceptor low bandgap copolymers based on benzothiadiazoles have been synthesized.⁵ Among them, some copolymers have been synthesized by using fluorenes,^{6,7} carbazoles,^{8,9} or dibenzosiloles^{10,11} as electron-donating comonomers. Usually, with such bridged phenylene units, two thiophene units had to be added on both ends of the benzothiadiazole core to obtain relatively planar copolymers; such a coplanar structure should allow good charge transport properties. Interestingly, this type of polymers has recently reached a PCE of 6.1% in BHJ photovoltaic devices.¹²

In parallel, Winnewisser et al. recently reported promising copolymers for use in optoelectronic applications based on electron-deficient dihydropyrrolo[3,4-*b*]pyrrole-1,4-dione (DPP).^{13,14} In addition to low energy bandgaps, the resulting copolymers have also demonstrated excellent charge transport properties. Consequently, good performances were afforded in both polymer solar cells and transistor devices.^{15,16}

However, most electronic devices suffer from a lack of long-term stability¹⁷ and relatively low performances that limit their industrial applications. Therefore, there is still a need for the development of new conjugated polymers. In this regard, we

present here the synthesis of new homopolymers and copolymers derived from 2,7-disubstituted germafluorenes. Huang et al. were the first to report the introduction (10% on a molar basis) of a similar unit (i.e., 3,6-dimethoxygermafluorene) in a random fluorene copolymer.¹⁸ Despite this recent study, it remains a challenge to investigate in more detail the structure–property relationships in homopolymers and copolymers based on germafluorene derivatives. The present work will also report the first utilization of such copolymers in FETs and photovoltaic devices.

Synthesis of the Monomers. The synthetic pathways for dibromo-di-*n*-octylgermane **3**, 2,7-dibromo-9,9-dibutyl-9-germafluorene **5**, 2,7-dibromo-9,9-dioctyl-9-germafluorene **6**, 2,7-bis(4',4',5',5'-tetramethyl-1',3',2'-dioxaborolan-2'-yl)-9,9-dibutyl-9-germafluorene **7**, and 2,7-bis(4',4',5',5'-tetramethyl-1',3',2'-dioxaborolan-2'-yl)-9,9-dioctyl-9-germafluorene **8** are described in Figure 1. The synthesis of the 4,4'-dibromo-2,2'-diiodobiphenyl **4** has already been reported in the literature.^{19,20} To obtain compound **3**, we modified a published procedure.²¹ First, a Grignard reagent (octylmagnesiumbromide **1**) was added to diphenyl germanium dichloride to obtain diphenyl-di-*n*-octylgermane **2**; then, this compound was treated with bromine to give the desired dibromo-di-*n*-octylgermane **3**. For the synthesis of compounds **5** and **6**, a modified procedure of that reported by Huang et al. was utilized.²² First, a dilithiation reaction on compound **4** was performed, followed by an addition of the germanium reagent. For the dilithiation reaction, it is very important to use exactly 2.05 equiv of *n*-butyllithium to make sure that all iodine atoms have reacted to avoid side reactions with the bromine atoms. The dilithiated product was then mixed with either the commercially available dichloro-di-*n*-butylgermane or the previously synthesized germanium-based reagent to afford compounds **5** and **6**, respectively. It is important to notice that the synthesis of compounds **5** and **6** has been done under Schlenk conditions. The reactions have been tried under standard inert conditions, but the yields were then much lower. Monomers **7** and **8** were synthesized using a

*Corresponding author. E-mail: mario.leclerc@chm.ulaval.ca.

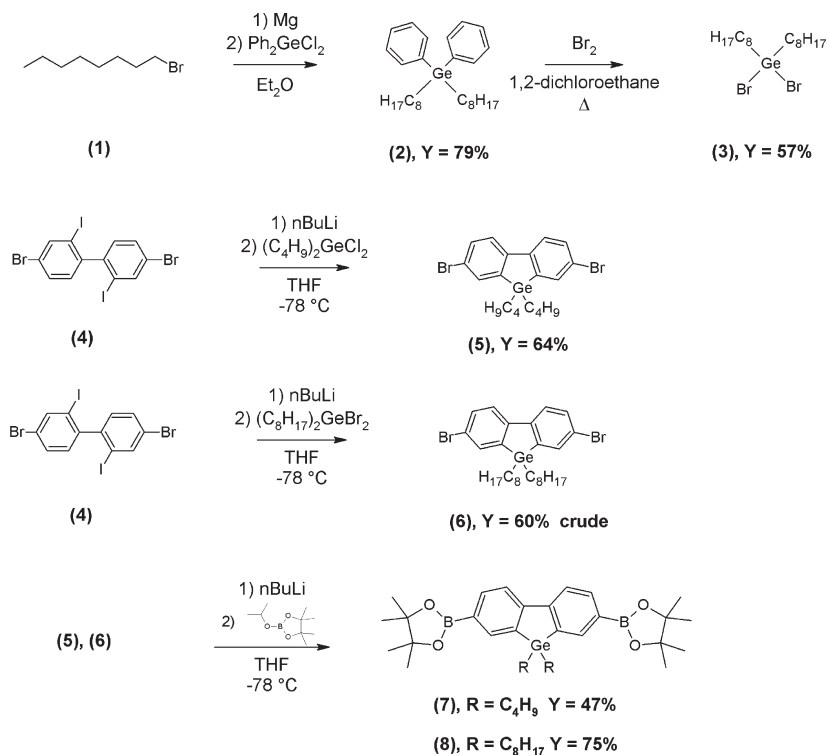


Figure 1. Synthesis of 2,7-disubstituted germafluorene monomers.

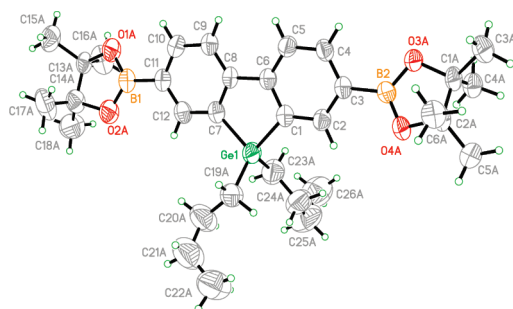


Figure 2. Single crystal structure of monomer 7.

dilithiation reaction on compounds **5** and **6**, followed by treatment with 2-isopropoxy-4,4,5,5-tetramethyl-1,3,2-dioxaborolane. For the results presented in this article, we used only germafluorenes with butyl or octyl alkyl chains, but it is possible to make different germanium reagents according to procedures described for the synthesis of compound **3**.

To confirm the structure of the two new monomers **7** and **8**, single crystals were grown from slow recrystallization in acetone. The two single crystal structures were determined and confirmed the success of these syntheses (Figures 2 and 3). These molecules are coplanar, as already published for some fluorene derivatives.²³

Synthesis of the Polymers. Five new conjugated polymers were synthesized according to Figure 4. **PGFDTDP** (**C₄**) and **PGFDTDP** (**C₈**) were obtained by the Suzuki cross-coupling polymerization²⁴ of compounds **7** and **8** with 3,6-bis(thiophen-5-yl)-2,5-dioctylpyrrolo[3,4-]pyrrole-1,4-dione **9** as comonomer. Monomer **9** was obtained by following a procedure reported in the literature.¹⁶ **PGFDTDP** (**C₈**) possesses a much better solubility than **PGFDTDP** (**C₄**), probably because of the presence of longer alkyl side chains. Furthermore, **PGFDTBT** was also synthesized by a Suzuki

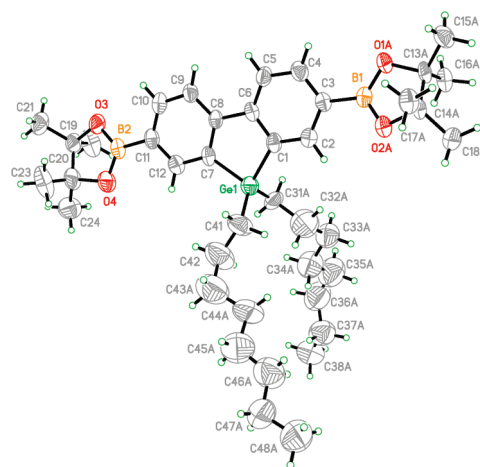


Figure 3. Single crystal structure of monomer 8.

cross-coupling polymerization between monomer **8** and 4,7-di(2-bromothiophen-5'-yl)-2,1,3-benzothiadiazole **10** using the same conditions reported for **PCDTBT**.⁸ The synthesis of the DTBT comonomer was done using an already known procedure.⁶ Homopolymer **PGF** (**C₄**) was synthesized using a Yamamoto coupling²⁵ of compound **5**, but the resulting polymer is insoluble. Because of the solubility problem with the homopolymer bearing butyl side chains, we wanted to make more soluble polygermafluorenes by using compound **6** under the same conditions. However, despite numerous attempts, compound **6** always showed some impurities making its polymerization impossible. Therefore, we synthesized a pseudo-homopolymer of germafluorene by making a Suzuki coupling between monomers **8** and **5** to obtain **PGF** (**C₄**, **C₈**). All polymers were washed with a Soxhlet apparatus with acetone and hexanes; then, the polymers were collected from the soluble fraction in chloroform.

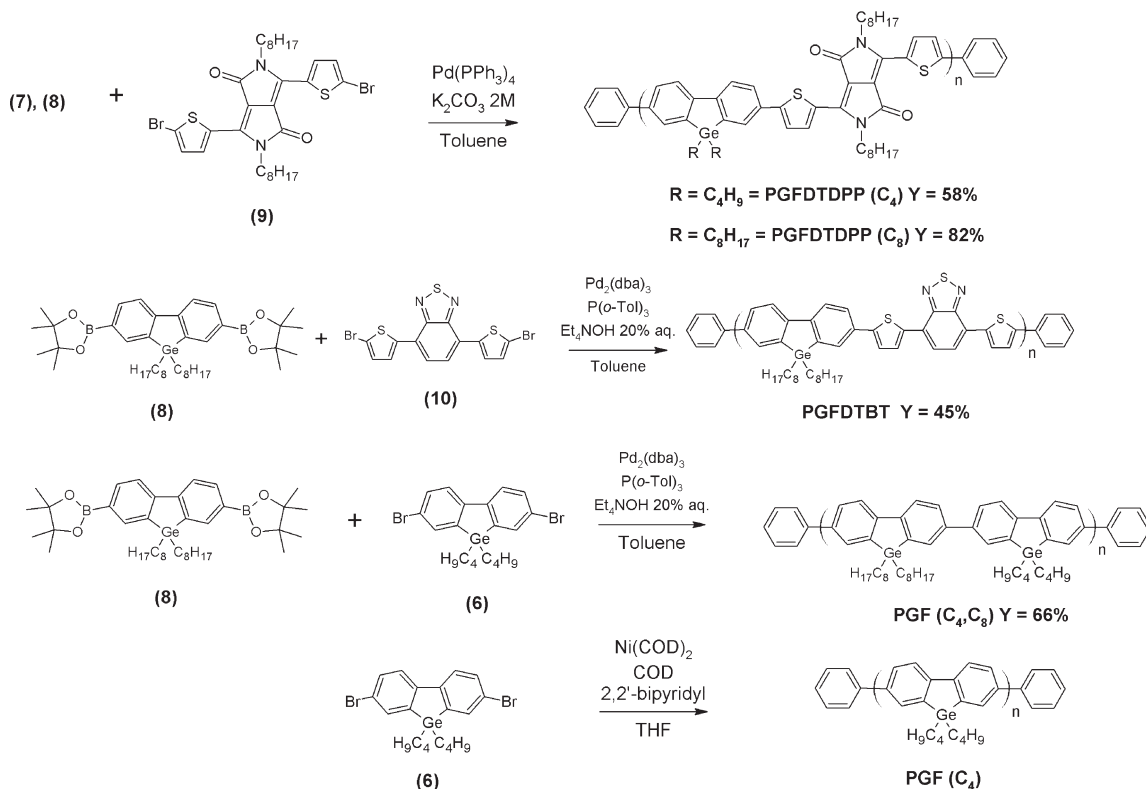


Figure 4. Synthesis of the germafluorene-based polymers.

Table 1. Number-Average Molecular Weight (M_n), Weight-Average Molecular Weight (M_w), Polydispersity Index (PDI), Glass-Transition Temperature (T_g), Degradation Temperature (T_d), and Optical and Electrochemical Properties of Polygermafluorene Derivatives

polymer	M_n (kg/mol)	M_w (kg/mol)	PDI	T_g ($^{\circ}\text{C}$)	T_d ($^{\circ}\text{C}$)	E_{HOMO} (eV)	E_{LUMO} (eV)	E_g^{elec} (eV)	E_g^{opt} (eV)
PGFDTDPP (C_4)	13	37	2.8	150	410	−5.38	−3.70	1.68	1.63
PGFDTDPP (C_8)	14	49	3.5	90	410	−5.38	−3.64	1.74	1.64
PGFDTBT	10	24	2.4	95	460	−5.58	−3.91	1.67	1.79
PGF (C_4, C_8)	10	19	1.9	130	430	−5.95	−2.82	3.13	2.95

Molecular Weights. All polymers were characterized by size exclusion chromatography (SEC) based on monodisperse polystyrene standards in trichlorobenzene at 140 $^{\circ}\text{C}$. Values obtained for SEC measurements are reported in Table 1. First, for PGFDTDPP (C_4), a number-average molecular weight (M_n) of 13 kg/mol was calculated with a polydispersity index of 2.8. In the case of PGFDTDPP (C_8), a number-average molecular weight of 14 kg/mol was measured with a polydispersity index of 3.5. For PGFDTBT, with a polymerization time of 6 h, we obtained a relatively low number-average molecular weight (M_n) of 10 kg/mol with a 2.4 polydispersity index. First attempts over 24 and 12 h resulted in a bimodal chromatogram. In the case of PGF (C_4, C_8), a first polymerization with $\text{Pd(PPh}_3)_4$ as catalyst resulted in a very low-molecular-weight polymer. Therefore, another catalytic system, $(\text{Pd}_2\text{dba}_3)$ with P(o-Tol)_3 , was tried, and a good number-average molecular weight (M_n) of 10 kg/mol was obtained with a polydispersity index of 1.9. The polymerization conditions for all of those molecular weights are described in the Supporting Information. It has been shown that the molecular weight of the material plays a significant role in the polymer optical and electrical properties.²⁶ Because those obtained in this study are relatively low, it could be interesting to find a way to increase them above 20 kg/mol, which is usually the target for better mechanical properties and better performances. Recently, Coffin et al. reported a new microwave-assisted method to synthesize high-molecular-weight polymers.²⁷ This could be an interesting way to improve the molecular weights.

Thermal Properties. To investigate the thermal stability and the thermal transitions of these polymers, thermogravimetric analysis (TGA) and differential scanning calorimetry (DSC) measurements were carried out. (See Table 1.) TGA analyses showed that all polymers had a good stability with degradation temperatures above 410 $^{\circ}\text{C}$. DSC experiments revealed that PGFDTDPP (C_4) has a high glass-transition temperature at 150 $^{\circ}\text{C}$ compared with 90 $^{\circ}\text{C}$ for PGFDTDPP (C_8). The difference between these two glass-transition temperatures is mainly due to the length of the alkyl side chains. In the case of PGFDTBT, measurements revealed a glass-transition temperature at 95 $^{\circ}\text{C}$. DSC analyses performed on PGF (C_4, C_8) showed a glass transition at 130 $^{\circ}\text{C}$. No melting transitions were observed.

Optical Properties. As shown in Figure 5, the optical properties were characterized by UV–vis absorption spectroscopy. For all polymers, no significant differences were observed between measurements made in solution and those made in the solid state. For PGF (C_4, C_8), the solid-state UV–vis absorption spectrum shows one absorption band at 380 nm. A bandgap of 2.95 eV is calculated from its absorption onset. The optical bandgap reported in the literature for the homopolymers based on fluorene (PF8) or dibenzosilole¹⁹ corresponds to a value of 2.93 eV, which is very similar to the bandgap obtained for PGF (C_4, C_8).

For PGFDTDPP (C_4) and PGFDTDPP (C_8), solid-state UV–vis absorption spectra show two absorption bands at 375 and 688 nm. From their respective absorption onset, the

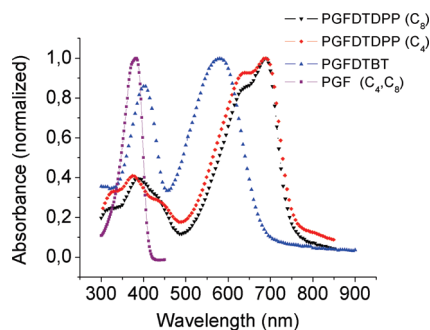


Figure 5. UV-vis absorption spectra of **PGF** (**C₄**, **C₈**), **PGFDTBT**, **PGFDTDP** (**C₄**), and **PGFDTDP** (**C₈**) as thin films.

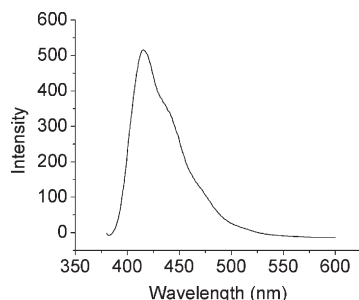


Figure 6. Fluorescence spectrum of **PGF** (**C₄**, **C₈**) in chloroform.

calculated optical bandgaps of **PGFDTDP** (**C₄**) and **PGFDTDP** (**C₈**) are 1.63 and 1.64 eV, respectively. Comparisons with fluorene-based analogs are difficult because there is a large range of data reported for those copolymers.¹⁴ Clearly, the optical properties of DPP-based copolymers are strongly affected by interchain interactions and resulting morphologies.

For **PGFDTBT**, two absorption bands at 403 and 580 nm are observed with an absorption onset at 693 nm. The optical bandgap for **PGFDTBT** is 1.79 eV. In the case of **PGFDTBT**, the optical bandgap obtained is lower than the optical bandgap of its homologues with fluorene (DiO-PFDTBT, APFO-3)^{28,29} and dibenzosilole (PSDTBT)¹⁰, which shows a bandgap of 1.9 and 1.85 eV, respectively. This slight red shift observed for **PGFDTBT** might be due to a better delocalization (π -stacking), probably indicating better intermolecular interactions.

To obtain further information about the pseudo-homopolymer, **PGF** (**C₄**, **C₈**), has also been characterized by fluorescence spectroscopy (Figure 6). Because polyfluorenes and poly(dibenzosiloles) show a blue emission, we investigated the fluorescence properties of this new polygermafluorene. As expected, **PGF** (**C₄**, **C₈**) shows a blue emission with a fluorescence maximum of 415 nm and a fluorescence quantum efficiency of 54% compared with 79% for poly[2,7-(9,9-dioctylfluorene)]³⁰ and 62% for poly[2,7-(9,9-dihexyldibenzosilole)].¹⁹

Electrochemical Properties. The HOMO and LUMO energy levels of all polymers were measured by cyclic voltammetry (CV). (See Table 1.) **PGFDTBT** shows one quasi-reversible oxidation process and one quasi-reversible reduction process. The HOMO and LUMO energy levels were then calculated from the oxidation and reduction onsets to give -5.58 and -3.91 eV, respectively. According to these energy levels, the electrochemical bandgap of **PGFDTBT** is 1.67 eV, compared with 1.79 eV obtained from optical measurements. As one can see in Figure 7, for **PGFDTDP** (**C₈**), one can distinguish two quasi-reversible oxidation processes and two

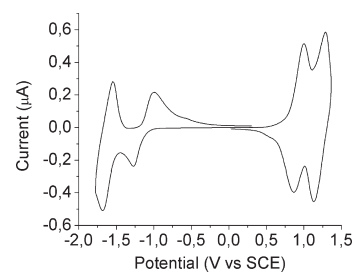


Figure 7. Cyclic voltammogram of **PGFDTDP** (**C₈**) in Bu_4NBF_4 /acetonitrile.

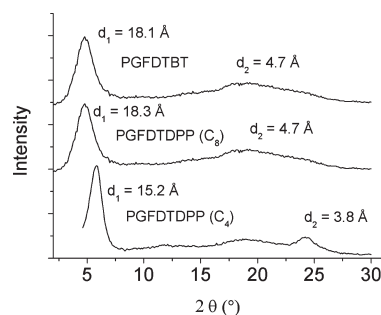


Figure 8. X-ray diffraction patterns of polygermafluorene derivatives.

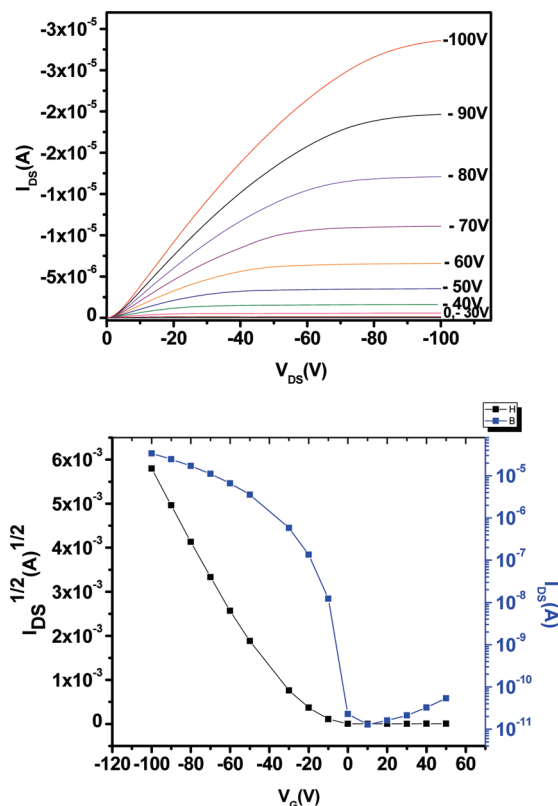


Figure 9. Output at different gate voltage (V_g) and transfer characteristics in the saturation regime at constant source-drain voltage ($V_{DS} = -100$ V) for FETs using **PGFDTDP** (**C₄**) films spin-coated on OTS-treated SiO_2/Si substrates.

quasi-reversible reduction processes. The HOMO and the LUMO energy levels were also calculated from the onset of the first oxidation and reduction processes and were found to be -5.38 and -3.64 eV. Therefore, the electrochemical bandgap of **PGFDTDP** (**C₈**) is 1.74 eV compared with 1.64 eV obtained from optical data. **PGFDTDP** (**C₄**) electrochemical

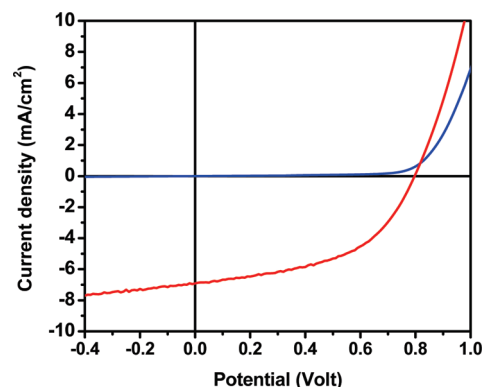
Table 2. Hole Carrier Mobility (μ), On/Off Ratios ($I_{\text{on}}/I_{\text{off}}$), Threshold Voltage (V_T), Open Circuit Voltage (V_{oc}), Short Circuit Current (I_{sc}), Fill Factor (FF), and Power Conversion Efficiency (PCE) for Poly(2,7-germafluorene) Derivatives

polymer	μ ($\text{cm}^2 \cdot \text{V}^{-1} \cdot \text{s}^{-1}$)	$I_{\text{on}}/I_{\text{off}}$	V_T (V)	V_{oc} (V)	I_{sc} ($\text{mA} \cdot \text{cm}^{-2}$)	FF	PCE %
PGFDTDPP (C₄)	0.04	1.0×10^6	−27	0.76	4.1	0.62	1.5
PGFDTDPP (C₈)	7.7×10^{-3}	3.6×10^5	−27	0.76	2.8	0.56	1.2
PGFDTBT	1.1×10^{-4}	1.8×10^4	−26	0.79	6.9	0.51	2.8

properties are very similar to those of its C₈ homologue. Therefore, **PGFDTDPP (C₄)** has two quasi-reversible oxidations and two quasi-reversible reductions processes. The HOMO and the LUMO energy levels of **PGFDTDPP (C₄)** were found to be −5.34 and −3.71 eV, resulting in an electrochemical bandgap of 1.63 eV. Finally, the cyclic voltammogram of **PGF (C₄, C₈)** shows one quasi-reversible oxidation process and one nonreversible reduction process. Because of the nature of the polymer, a large bandgap was expected. The HOMO and LUMO energy levels were calculated to be −5.95 and −2.82 eV, giving an electrochemical band gap of 3.13 eV. All of these polymers have a good air stability because their HOMO energy level is below −5.27 eV.³¹

X-ray Diffraction Analyses. X-ray diffraction (XRD) analyses on powders were performed for all low bandgap copolymers (Figure 8). **PGFDTBT** and **PGFDTDPP (C₈)** show a peak at $d_1 \approx 18$ Å, whereas **PGFDPP (C₄)** shows a peak at $d_1 \approx 15$ Å. The difference between the d_1 distance of **PGFDTDPP (C₄)** and the d_1 distance of **PGFDTDPP (C₈)** and **PGFDTBT** is probably due to the length of the alkyl side chains. Effectively, it is fair to assume that this d_1 value is attributed to the distance between polymer main chains.³² Also, **PGFDTBT** and **PGFDTDPP (C₈)** show a weak and flat diffraction peak at $d_2 \approx 4.7$ Å compared with a weak and sharper diffraction peak at $d_2 \approx 3.8$ Å for **PGFDTDPP (C₄)**. This d_2 value can be attributed to the distance between stacked coplanar main chains. The presence of shorter *n*-butyl side chains seems to improve the packing of the polymer by decreasing the distance between each main chain. When comparing those polymers, one can suppose that **PGFDTDPP (C₄)** has a better organization than **PGFDTDPP (C₈)** and **PGFDTBT**.

Field-Effect Transistors. To investigate the potential of these new copolymers in plastic electronics, FETs were fabricated and tested. First, 40 nm thick polymer films were deposited on OTS-treated SiO₂/Si substrates by spin-coating a 4 mg/mL chloroform solution of the polymers. Then, films were heated under nitrogen at 55 °C for 10 min or annealed at a temperature of 100, 150, or 200 °C for 30 min. The source and drain electrodes were defined by thermally evaporating 700 Å of gold through a shadow mask with a channel width of 2600 μm and a channel length of 45 μm on top of the organic thin films forming top-contact geometry transistors. All electrical measurements were carried out at room temperature under ambient conditions. Further information on the surface treatments can be found in the Supporting Information section. Interesting performances were obtained with **PGFDTDPP (C₄)** and **PGFDTDPP (C₈)** when annealed at 150 °C for 30 min. **PGFDTDPP (C₄)** shows a hole mobility of $0.04 \text{ cm}^2 \cdot (\text{V} \cdot \text{s})^{-1}$ with an $I_{\text{on}}/I_{\text{off}}$ ratio of 1.0×10^6 and a threshold voltage of −27 V. (See Figure 9.) Then, for **PGFDTDPP (C₈)**, we calculated a hole mobility of $7.7 \times 10^{-3} \text{ cm}^2 \cdot (\text{V} \cdot \text{s})^{-1}$ with an $I_{\text{on}}/I_{\text{off}}$ ratio of 3.6×10^5 and a threshold voltage of −27 V. **PGFDTBT** has also been tested in FETs and shows a hole mobility of $1.07 \times 10^{-4} \text{ cm}^2 \cdot (\text{V} \cdot \text{s})^{-1}$ with an $I_{\text{on}}/I_{\text{off}}$ ratio of 1.81×10^4 and a threshold voltage of −26 V. It is well known that the organization of the polymer is one of the important criteria to obtain good field-effect mobility. Powder XRD analyses showed that **PGFDTDPP (C₄)** was probably the most

**Figure 10.** J – V curves of **PGFDTBT** solar cell. Under illumination of AM 1.5 G in red and dark curve in blue.

promising polymer because of its better π -stacking. This statement is confirmed by the characterization of FET devices; this material shows a higher hole mobility.

Polymer Solar Cells. BHJ PCs, using a sandwiched structure of glass/ITO/PEDOT–PSS/polymer–PC₇₀BM/LiF/aluminum, were prepared on commercial ITO-coated glass substrate of 38 \times 38 mm with a sheet resistance of ca. 15 Ω /square. Prior to use, the substrates were ultrasonicated in deionized water, acetone, and isopropanol. ITO substrates were coated with a thin film (40 nm) of poly(3,4-ethylenedioxythiophene)/poly(styrenesulfonate) (PEDOT/PSS) and then dried at 120 °C for 60 min. A blend of [6,6]-phenyl C₇₀-butyric acid methyl ester (PC₇₀BM) and polymer was solubilized in chloroform for **PGFDTDPP (C₄)** and **PGFDTBT (C₈)** for 24 h and in ODCB for **PGFDTBT** for 4 days and filtered through a 1 μm poly(tetrafluoroethylene) (PTFE) filter, and the films were finally spin-coated on the substrates. The resulting films were dried for at least 24 h. Finally, the devices were put under reduced pressure at room temperature for 12 h. The devices were completed by deposition of 20 nm of lithium fluoride and 1200 nm of aluminum. A summary of the results obtained is shown in Table 2. **PGFDTDPP (C₄)**-based PCs demonstrated a current density of $4.1 \text{ mA} \cdot \text{cm}^{-2}$, a fill factor of 0.62, and an open circuit voltage (V_{oc}) of 0.76 V, leading to a PCE of 1.5%. In the case of **PGFDTDPP (C₈)**, we obtained a current density of $2.8 \text{ mA} \cdot \text{cm}^{-2}$, a fill factor of 0.56, and an open circuit voltage of 0.76 V. As a result, a PCE of 1.2% was achieved. The higher hole mobility in the first copolymer may explain differences in the power conversion efficiencies. Similar polymeric structures using a fluorene-DPP backbone have been reported recently in the literature.¹⁴ Those polymers showed V_{oc} values of about 0.74 to 0.78 V and PCE of about 0.78 to 0.88%. V_{oc} values obtained for PGFDTDPPs are about the same, but the PCE seems to be a little higher. Finally, the J – V curve of **PGFDTBT** shows a current density of $6.9 \text{ mA} \cdot \text{cm}^{-2}$, a fill factor of 0.51, and an open circuit voltage of 0.79 V. (See Figure 10.) A PCE of 2.8% was obtained with **PGFDTBT**. A lot of studies have already been reported in the literature on fluorene-DTBT and silafluorene-DTBT polymers for photovoltaic applications. Indeed, fluorene-DTBT-based PCs were reported in 2004 with V_{oc} values between 0.95 and 1.01 V and PCE between

2.10 and 2.24%.^{28,33} Recent optimizations on fluorene-DTBT polymers allowed a PCE of 4.2% with a V_{oc} of 0.99 V.⁷ A silafluorene-DTBT polymer has also been reported with a PCE of 5.4% and a V_{oc} of 0.90 V.¹¹ When comparing those results with the present ones, one can effectively suppose that there is no significant improvement of either the PCE or the V_{oc} when using a germafluorene backbone. However, as it happened for other classes of polymers, better performances could be expected by optimizing the morphology of the BHJ solar cells.

Conclusions

In this study, we presented the synthesis and characterization of new germafluorene derivatives. Homopolymers and alternating copolymers have been synthesized and characterized for the first time. All polymers are thermally stable up to 410 °C and present relatively good molecular weights. These germafluorene-based polymers exhibit bandgaps ranging from 3.0 to 1.6 eV. Accordingly, it is possible to fine-tune the HOMO and LUMO energy levels. Preliminary studies in FETs and PCs showed very promising results (hole mobility up to $0.04 \text{ cm}^2 \cdot \text{V}^{-1} \cdot \text{s}^{-1}$ and power conversion up to 2.8%) for application in plastic electronics. In this regard, new device configurations as well as new germafluorene-based polymers will be investigated. It is believed that these new heterocycles should bring new synthetic tools for the future design of conjugated polymers with optimized properties.

Acknowledgment. This work was supported by grants from the Natural Sciences and Engineering Research Council (NSERC) of Canada. The authors acknowledge Konarka Technologies (S. Rodman) for SEC measurements.

Supporting Information Available: Experimental details, syntheses of the monomers and polymers, instrumentation, and characterization procedures. This material is available free of charge via the Internet at <http://pubs.acs.org>.

References and Notes

- (1) Allard, S.; Forster, M.; Souharce, B.; Thiem, H.; Scherf, U. *Angew. Chem., Int. Ed.* **2008**, *47*, 4070–4098.
- (2) (a) Chen, H.-Y.; Hou, J.; Zhang, S.; Liang, Y.; Yang, G.; Yang, Y.; Yu, L.; Wu, Y.; Li, G. *Nat. Photonics* **2009**, *3*, 649–653. (b) Brabec, C. J.; Sariciftci, N. S.; Hummelen, J. C. *Adv. Funct. Mater.* **2001**, *11*, 15–26. (c) Coakley, K. M.; McGehee, M. D. *Chem. Mater.* **2004**, *16*, 4533–4542.
- (3) (a) Zhang, M.; Tsao, H. N.; Pisula, W.; Yang, C.; Mishra, A. K.; Mullen, K. *J. Am. Chem. Soc.* **2007**, *129*, 3472–3473. (b) Tsao, H. N.; Cho, D.; Andreasen, J. W.; Rouhanipour, A.; Breiby, D. W.; Pisula, W.; Müllen, K. *Adv. Mater.* **2009**, *21*, 209–212.
- (4) Peet, J.; Kim, J. Y.; Coates, N. E.; Ma, W. L.; Moses, D.; Heeger, A. J.; Bazan, G. C. *Nat. Mater.* **2007**, *6*, 497–500.
- (5) Chen, J.; Cao, Y. *Acc. Chem. Res.* **2009**, *42*, 1709–1718.
- (6) Svensson, M.; Zhang, F.; Veenstra, S. C.; Verhees, W. J. H.; Hummelen, J. C.; Kroon, J. M.; Inganäs, O.; Andersson, M. R. *Adv. Mater.* **2003**, *15*, 988–991.
- (7) Slooff, L. H.; Veenstra, S. C.; Kroon, J. M.; Moet, D. J. D.; Sweelssen, J.; Koetse, M. M. *Appl. Phys. Lett.* **2007**, *90*, 143506–3.
- (8) Blouin, N.; Michaud, A.; Leclerc, M. *Adv. Mater.* **2007**, *19*, 2295–2300.
- (9) Blouin, N.; Michaud, A.; Gendron, D.; Wakim, S.; Blair, E.; Neagu-Plesu, R.; Belletete, M.; Durocher, G.; Tao, Y.; Leclerc, M. *J. Am. Chem. Soc.* **2008**, *130*, 732–742.
- (10) Boudreault, P.-L. T.; Michaud, A.; Leclerc, M. *Macromol. Rapid Commun.* **2007**, *28*, 2176–2179.
- (11) Wang, E.; Wang, L.; Lan, L.; Luo, C.; Zhuang, W.; Peng, J.; Cao, Y. *Appl. Phys. Lett.* **2008**, *92*, 033307.
- (12) Park, S. H.; Roy, A.; Beaupre, S.; Cho, S.; Coates, N.; Moon, J. S.; Moses, D.; Leclerc, M.; Lee, K.; Heeger, A. J. *Nat. Photonics* **2009**, *3*, 297–302.
- (13) (a) Zou, Y.; Gendron, D.; Neagu-Plesu, R.; Leclerc, M. *Macromolecules* **2009**, *42*, 6361–6365. (b) Bürgi, L.; Turbiez, M.; Pfeiffer, R.; Biewald, F.; Kirner, H.-J.; Winnewisser, C. *Adv. Mater.* **2008**, *20*, 2217–2224. (c) Bijleveld, J. C.; Zoombelt, A. P.; Mathijssen, S. G. J.; Wienk, M. M.; Turbiez, M.; de Leeuw, D. M.; Janssen, R. A. J. *J. Am. Chem. Soc.* **2009**, *131*, 16616–16617.
- (14) (a) Zhou, E.; Yamakawa, S.; Tajima, K.; Yang, C.; Hashimoto, K. *Chem. Mater.* **2009**, *21*, 4055–4061. (b) Huo, L.; Hou, J.; Chen, H.-Y.; Zhang, S.; Jiang, Y.; Chen, T. L.; Yang, Y. *Macromolecules* **2009**, *42*, 6564–6571.
- (15) Wienk, M. M.; Turbiez, M.; Gilot, J.; Janssen, R. A. J. *Adv. Mater.* **2008**, *20*, 2556–2560.
- (16) Zou, Y.; Gendron, D.; Badrou-Aïch, R.; Najari, A.; Tao, Y.; Leclerc, M. *Macromolecules* **2009**, *42*, 2891–2894.
- (17) List, E. J. W.; Guentner, R.; Scanducci de Freitas, P.; Scherf, U. *Adv. Mater.* **2002**, *14*, 374–378.
- (18) Chen, R.; Zhu, R.; Zheng, C.; Liu, S.; Fan, Q.; Huang, W. *Sci. China, Ser. B: Chem.* **2009**, *52*, 212–218.
- (19) Chan, K. L.; McKiernan, M. J.; Towns, C. R.; Holmes, A. B. *J. Am. Chem. Soc.* **2005**, *127*, 7662–7663.
- (20) Usta, H.; Lu, G.; Facchetti, A.; Marks, T. J. *J. Am. Chem. Soc.* **2006**, *128*, 9034–9035.
- (21) Miller, R. D.; Sooriyakumaran, R. *J. Polym. Sci., Part A: Polym. Chem.* **1987**, *25*, 111–125.
- (22) Chen, R. F.; Fan, Q. L.; Zheng, C.; Huang, W. *Org. Lett.* **2006**, *8*, 203–205.
- (23) Ranger, M.; Leclerc, M. *Macromolecules* **1999**, *32*, 3306–3313.
- (24) Miyaura, N.; Suzuki, A. *Chem. Rev.* **1995**, *95*, 2457–2483.
- (25) Yamamoto, T. *Synlett* **2003**, 425–450.
- (26) Zen, A.; Pflaum, J.; Hirschmann, S.; Zhuang, W.; Jaiser, F.; Asawapirom, U.; Rabe, J. P.; Scherf, U.; Neher, D. *Adv. Funct. Mater.* **2004**, *14*, 757–764.
- (27) Coffin, R. C.; Peet, J.; Rogers, J.; Bazan, G. C. *Nat. Chem.* **2009**, *1*, 657–661.
- (28) Zhou, Q.; Hou, Q.; Zheng, L.; Deng, X.; Yu, G.; Cao, Y. *Appl. Phys. Lett.* **2004**, *84*, 1653–1655.
- (29) Inganäs, O.; Zhang, F.; Andersson, M. R. *Acc. Chem. Res.* **2009**, *42*, 1731–1739.
- (30) Ranger, M.; Rondeau, D.; Leclerc, M. *Macromolecules* **1997**, *30*, 7686–7691.
- (31) (a) Thompson, B. C.; Kim, Y. G.; Reynolds, J. R. *Macromolecules* **2005**, *38*, 5359–5362. (b) Leeuw, D. M.; Simenon, M. M. J.; Brown, A. R.; Einerhand, R. E. F. *Synth. Met.* **1997**, *87*, 53–59.
- (32) (a) Grell, M.; Bradley, D. D. C.; Ungar, G.; Hill, J.; Whitehead, K. S. *Macromolecules* **1999**, *32*, 5810–5817. (b) Chen, S. H.; Su, A. C.; Chen, S. A. *J. Phys. Chem. B* **2005**, *109*, 10067–10072.
- (33) Inganäs, O.; Svensson, M.; Zhang, F.; Gadisa, A.; Persson, N. K.; Wang, X.; Andersson, M. R. *Appl. Phys. A: Mater. Sci. Process.* **2004**, *79*, 31–35.